Substrate Effect on Hydrogen Evolution Reaction in Two-Dimensional Mo2C Monolayers

Sujin Lee
Dongguk University-Seoul
Byungjoon Min
Chungbuk National University
Junhyeok Bang (jbang@cbnu.ac.kr)
Chungbuk National University

Research Article

Keywords: electrocatalytic hydrogen evolution reaction, Mo2C monolayer, graphene, electrocatalysis

Posted Date: October 11th, 2021

DOI: https://doi.org/10.21203/rs.3.rs-954700/v1

Substrate Effect on Hydrogen Evolution Reaction in Two-Dimensional Mo_2C Monolayers

Sujin Lee[1], Byungjoon Min[2,3], and Junhyeok Bang[2,3*]

[1]*Department of Energy and Materials Engineering, Dongguk University-Seoul, Seoul, 04620, Korea*

[2]*Department of Physics, Chungbuk National University, Cheongju 28644, Republic of Korea*

[3]*Research Institute for Nanoscale Science and Technology, Cheongju 28644, Republic of Korea*

Abstract

The physical and chemical properties of atomically thin two-dimensional (2D) materials can be modified by the substrates. In this study, the substrate effect on the electrocatalytic hydrogen evolution reaction (HER) in 2D Mo_2C monolayers was investigated using first principles calculations. The isolated Mo_2C monolayer shows large variation in HER activity depending on hydrogen coverage: it has relatively low activity at low hydrogen coverage but high activity at high hydrogen coverage. Ag, Au, Cu, and graphene were used as substrates to study the substrate effect. While the effects of the Au and graphene substrates on the HER activity are insignificant, Ag and Cu substrates improve the HRE activity, especially at low hydrogen coverage, by modifying the valence electrons in the Mo_2C layer; therefore, the HER activity of the Mo_2C monolayer becomes high for any hydrogen coverage. Our results suggest that, in two-dimensional electrocatalysis, the substrate has a degree of freedom to tune the catalytic activity.

*Corresponding authors: J. Bang (jbang@cbnu.ac.kr)

Introduction

There are various clean and renewable energy resources that are alternatives to fossil fuels, such as solar, wind, tide, and biomass energy. However, they suffer from intermittent availability, and thus, efficient energy conversion and storage systems are necessary for these alternatives [1,2]. Hydrogen has been considered a promising candidate for energy storage. It is clean and renewable with an energy storage density much higher than that of batteries, which makes it suitable for application in large-scale production facilities [3,4]. A hydrogen evolution reaction (HER) in water involves proton reduction and concomitant evolution of hydrogen molecule; it is an endothermic reaction with an additional kinetic energy barrier in intermediate processes. In this regard, catalysis to lower the kinetic energy barrier is crucial for efficient hydrogen production [5,6]. Although noble metals like Pt and Pd show high catalytic performance, they cannot be used in large-scale industrial applications owing to their scarcity [5,7,8]. Therefore, the development of low-cost and high-performance HER electrocatalysts has emerged an urgent issue for renewable and clean energy. In addition, HER is important for a variety of electrochemical processes either than energy storage, such as hydrogen fuel cells, electrodeposition, and the corrosion of metals in acids [9,10].

Two-dimensional (2D) materials have emerged as potential HER catalysts owing to their large surface areas and earth-abundant elements. To date, several 2D systems, such as graphene and transition metal dichalcogenides (TMDs), have been studied for HER electrocatalysis [11-16], and the results showed that the HER performance can be improved by intrinsic defects, doping, surface functionalization, strain engineering, phase regulation, and grain boundaries [17-24]. Recently, the transitional-metal carbide/nitride monolayer (MXene) was experimentally discovered as a new type of 2D material [25-27]. The chemical formula of MXene is $M_{n+1}X_n$, where M is a transition metal and X is C or N. In contrast to TMDs, MXene is intrinsically a metal

in the 1T and 2H phases and has a high density of states near the Fermi level. These features are a prerequisite for excellent HER activity, and the electrocatalytic properties of MXene have been studied [28-30]. For example, the basal planes of Mo_2C can be catalytically activated by functionalization with –O, –H, –OH, and –F groups in contrast to 2H-MoS_2 [31]. Among these functional groups, the highest HER performance was observed for the samples functionalized with the –O group [31,32]. The catalytic activity of the Mo_2C 2H phase can be enhanced by Co doping owing to the increase in the density of states at the Fermi level [33], and Mo_2C co-doped with N and S also shows a high HER performance [34,35].

2D materials in electrocatalytic cells are placed on a metal substrate, which acts as an electrode. Because 2D systems are atomically thin unlike bulk materials, the substrate inevitably affects their surface chemistry. The effect may be considered insignificant because the catalytic reactions occur directly on the 2D materials, not on the substrate. However, this is not true: one famous counterintuitive example is the strong modification of chemical reactions in ultrathin oxide films on metal substrates, where the electron tunneling from the substrate plays a crucial role [36-38]. As such, it may be possible to optimize HER activity using substrates. Although there have been significant studies on chemically modifying MXenes and their HER electrocatalytic properties, the substrate effect on these materials is not yet understood. In this study, using density functional theory (DFT) calculations, we investigated the substrate effect on the HER activity of MXene. Here, we focus on Mo_2C as a typical example of MXene and consider several metal substrates such as Ag, Au, Cu, and graphene. Based on the Sabatier principle, we estimated the catalytic HER activity using the calculated reaction free energy for hydrogen adsorption. Our results show that the HER activity of the isolated Mo_2C monolayer is higher than those of the isolated Ag and Au metal catalysts, but is comparable to that of the Cu catalyst. While the substrate

effects of the Au and graphene were not significant, the HER activity of Mo_2C on the Ag and Cu substrates was improved to be greater than that of Cu. These improvements are caused by the modification of the effective charge of Mo atoms and consequent reduction of the Coulomb attraction between Mo_2C and hydrogen. The results suggest that the substrate can be used for fine-tuning HER activity in two-dimensional electrocatalysis.

Calculation Methods

The optimized geometries and relevant total energies were calculated using DFT calculations [39,40] with the Perdew-Burke-Ernzerhof exchange-correlation functional [41], as implemented in the Vienna *ab initio* simulation package [42]. The projected augmented wave potentials were used to represent the ion cores [43,44]. The wave functions were expanded in a plane wave basis set up to a cut-off energy of 400 eV. To model the Mo_2C monolayer [see Fig. 1(a)], we used a periodic supercell containing 48 atoms ($4 \times 2\sqrt{3}$ unit cells). For the Ag, Au, Cu, and Pt substrates, we employed periodic slab models containing six atomic layers along the (001) direction. In all the calculations, the slabs were separated by a vacuum gap of at least 20 Å. The 2×2×1 Monkhorst-Pack k-point mesh was used for Brillouin-zone integration. We used optimized lattice parameters for the Mo_2C and substrates and the lattice parameters of the Mo_2C monolayer for the Mo_2C on a substrate [Fig. 1(b)]. In all the cases, the lattice mismatches were below 10%, and the effect of the lattice mismatches was small because hydrogen atoms are directly bonded to Mo_2C, not the substrates. We fixed the positions of the atoms in the two bottom layers of the substrates, and the atomic positions of the other atoms were fully relaxed until the residual forces were less than 0.01 eV/Å.

The HER activity was measured using the variation of the reaction free energy in hydrogen adsorption (ΔG), represented by

$$\Delta G = \Delta E_H + \Delta ZPE - T\Delta S,$$

where ΔE_H, ΔZPE, and ΔS are the changes in the DFT total energies, zero-point energy, and entropy of a hydrogen atom when absorbing an electrocatalyst from an H_2 molecule, respectively, and T is the system temperature, which is usually room temperature. Here, ($\Delta ZPE - T\Delta S$) is set to 0.24 eV [28,45-47]. ΔE_H can be calculated using either

$$\Delta E_H = E(X+nH) - E(X+(n-1)H) - E(H_2)/2$$

for the individual process or

$$\Delta E_H = [\, E(X+nH) - E(X) - nE(H_2)/2] \,/\, n$$

for the average process [47]. Here, $E(H_2)$, $E(X)$, and $E(X+nH)$ are the total energies of the H_2 molecule, electrocatalyst X, and electrocatalyst X with n hydrogen atoms, respectively. The difference between the two is qualitatively insignificant; therefore, we used the latter only.

Results and Discussion

It is well known that the catalytic activity of a material is strongly correlated with the reactant–material bond strength: a volcano-shaped graph is formed when the activity is plotted with the bond strength [48-50]. This is explained by the Sabatier principle, which states that catalytic activity is high when the bond strength is neither too strong nor too weak. If the bond strength is too weak, the surface cannot activate the catalytic reaction. If the bond strength is too

strong, the product fails to dissociate; the optimal bond strength balances the two extremes. In the HER, this principle can be quantified by the reaction free energy of hydrogen adsorption ΔG [28,45], as defined above. Previous experiments have shown that an electrocatalyst with a ΔG close to the optimal value exhibits a high exchange current density, which is a measure of the electrocatalytic activity, and the exchange current density exponentially decreases as ΔG deviates from the optimal value [45,48,51]. ΔG has been a reasonable descriptor of the HER activity for a wide variety of metals and alloys and has been applied in the design of highly efficient catalysts [52,53]. Parsons suggested that the optimum value was approximately $\Delta G = 0$ [48]. Recent theoretical and experimental results have reported that the optimal ΔG (approximately −0.4 eV) is slightly smaller than zero in alkaline electrolytes [51].

Before we discuss the Mo_2C monolayers, we consider the HER activity of metal substrates such as Ag, Au, Cu, Pt, and graphene. For the substrates, only the (001) surface was considered. Figure 2(a) shows the ΔG of the metal substrates with respect to the coverage of the hydrogen absorbed on the surfaces. The coverage is defined as the ratio of the number of absorbed H atoms to the total number of possible absorption sites. The Pt substrate had the smallest ΔG for each H coverage, and the ΔG for each H coverage increased in the order of Cu, Ag, Au, and graphene. The ranges of the ΔG were from −0.37 to −0.02 eV, from 0.14 to 0.30 eV, from 0.41 to 0.53 eV, from 0.50 to 0.97 eV, and from 0.89 to 1.53 eV, for Pt, Cu, Ag, Au, and graphene, respectively. These results are in good agreement with previous findings [45,51]. In the graphene substrate, ΔG abruptly decreases to −0.79 and 0.54 eV at the two high coverages of 0.75 and 1.0, respectively. This is related to the qualitative change in the C π-bonding network accompanied by the metal-to-insulator transition [54-57]. In this regard, we exclude the two results in Fig. 2, because an insulator

cannot be an electrocatalyst. Although the ΔG of both Pt and Cu were close to zero, the experiments clearly show that Pt is the better HER activity catalyst compared to Cu [45,51]. The results indicate that the optimal ΔG is close to, but smaller than zero. Therefore, in the following, we set the optimal value to the average ΔG of Pt (−0.18 eV), which is represented by the horizontal lines in Fig. 2 (a) and (b). This indicates as the ΔG approaches the optimal value, the catalysis of HER activity increases.

Next, we consider the HER activity, i.e., ΔG, of Mo_2C. To date, many studies have considered the Mo_2C 1T phase, despite it being less stable than the 2H phase [58,59]. Here, we focused on the 2H phase. As shown in Fig. 1(a), Mo_2C has three absorption sites for hydrogen atoms, such as the top of a hexagonal center (TH), a C atom (TC), and a Mo atom (TM) [see Fig. 1(a)]. The H atom is the most stable at the TH site, and the energy increases by 0.20 eV at the TC site. The TM site is unstable, and the H atom moves to the stable TH site during ionic relaxation. In high H coverages, the TH sites of H atoms also have lower energies than the other sites. In this regard, we calculated the ΔG of the TH sites, and the results are shown in Figs. 2(a) and (b). For the isolated Mo_2C monolayer, ΔG varies from −0.71 eV for low hydrogen coverage (0.0625) to −0.37 eV for full hydrogen coverage (1.0).

To directly compare the HER activity of Mo_2C with those of the metal substrates, we plotted the volcano-shaped HER activity with the peak located at the optimal ΔG in Fig. 3. The ΔG of Cu, Ag, Au, and graphene were all positive and located on the right of the optimal value. The HER activity of the Cu substrate was expected to be higher than the other substrate except Pt. The results of the graphene substrate are not shown in Fig. 3 because it had very large ΔG values, that is, very low HER activity. As discussed above, the ΔG values of Mo_2C were smaller than the

optimal value; thus, the HER activity (black line) is shown on the left side of the optimal line in Fig. 3. The HER activity of Mo_2C was expected to be higher than that of Ag and Au, but comparable to that of Cu. The HER activity of Mo_2C was broader than that of Cu, and the HER activity was lower with low H coverage, but it was higher for high H coverage.

The HER activity can be affected by the metal substrate of Mo_2C. Figure 1(b) shows the atomic structure of Mo_2C on a substrate: the Mo_2C was placed on the (001) surface of the substrate. There was no strong bonding between the Mo_2C and substrates, but a heterostructure was formed by a weak dispersive interaction. The atomic structures indicated that the physical properties of Mo_2C were not significantly altered by the substrates. Using these structures, we calculated the ΔG of Mo_2C on Cu, Ag, Au, and graphene substrates, and the results are shown in Figs. 2(a) and (b). The ΔG values for all cases are distributed in the range from -0.74 to -0.35 eV, which is similar to the range of the isolated Mo_2C case (-0.71 ~ -0.37 eV). These results indicate that Mo_2C is dominant in determining ΔG because the H atoms directly bond to Mo_2C, and the substrate effects are secondary. However, there are some ΔG differences that are attributable to the substrate. For Mo_2C on Au and graphene substrates, the changes in ΔG with H coverage are similar to those of the isolated Mo_2C monolayer, which implies that the effects of the two substrates are negligible. On the other hand, the variation was significantly reduced for Mo_2C on Cu and Ag substrates. Note that, while the ΔG for high coverages is similar to that of the Mo_2C monolayer, the ΔG for low coverage increases on the Cu and Ag substrates. This ΔG change modifies the HER activity. As shown in Fig. 3, the overall HER activity was better than that observed in the isolated Cu substrates, as the ΔG approaches the optimal value for all H coverages. Thus, the HER activity of 2D Mo_2C can be adjusted by the substrate.

The increase in ΔG for low H coverage on the Cu and Ag substrates indicates the weakening of the bond strength between Mo_2C and H. To understand the change in the bond strength, we performed Bader charge analysis, as shown in Table 1. In the Mo_2C without a substrate, some of the six valence electrons in the Mo atom are transferred to the C atoms, resulting in positively charged Mo ions and negatively charged C ions. Bader charge analysis shows quantitative changes in the valence electrons. Each Mo atom in Mo_2C has 5.434 valence electrons, which implies that each Mo atom loses 0.566 electrons; thus, the effective charge of the Mo ion becomes +0.566. When an H atom is absorbed in the TH site of Mo_2C, the electrons in the three nearest neighboring Mo atoms are also transferred to the H atom, and the effective charges of the Mo and H atoms become +0.658 and -0.453, respectively. The number of transferred electrons 0.276 [$= 3 \times (0.658 - 0.566)$] from the three Mo atoms is less than the electron gains of the H atom, because electrons from other Mo atoms are also transferred. The charge imbalance induces Coulomb attraction between the Mo and H atoms, which increases the bond strength.

The substrates modify the charge imbalance, and thus the Coulomb attraction. For the Mo_2C on the Ag and Cu substrates, the valence electrons in the Mo atoms increased to 5.502 and 5.492, respectively, compared to the isolate Mo_2C (5.434). This implies that the substrates donate electrons to the Mo_2C layer. As such, the effective charge of the Mo atoms is reduced to +0.498 and +0.508 on the Ag and Cu substrates, respectively. The reduction also affects the effective charge of the Mo atoms after H absorption, as shown in Table 1, while the effective charges of the H atoms (~ -0.45) remain nearly the same for the different substrates. In this regard, the Coulomb attraction is weakened for the Mo_2C on the Ag and Cu substrates, thereby increasing ΔG. On the other hand, for the Mo_2C on the Au substrates, the electric charges of the Mo atoms are similar to those in the isolated Mo_2C; thus, the variations of ΔG shown in Fig. 2 are also similar to those of

the isolated Mo_2C. Thus, the charge redistribution caused by the substrates can affect the HER activity of the 2D Mo_2C.

Summary

In summary, we investigated the substrate effect on the HER activity of 2D Mo_2C and compared its activity with that of metal catalysts such as Ag, Cu, Au, and graphene. The HER activity of the isolated Mo_2C exhibits relatively large variation depending on the hydrogen coverage, showing low activity at low hydrogen coverage and high activity at high hydrogen coverage. While the substrate effect is not significant, we have shown that Ag and Cu substrates can tune the HER activity of Mo_2C, especially at low hydrogen coverage, such that HER activity becomes high for all H coverages. Our results suggest a method for tuning the HER activity of two-dimensional electrocatalysis.

ACKNOWLEDGMENT

This research was supported by Chungbuk National University Korea National University Development Project (2020).

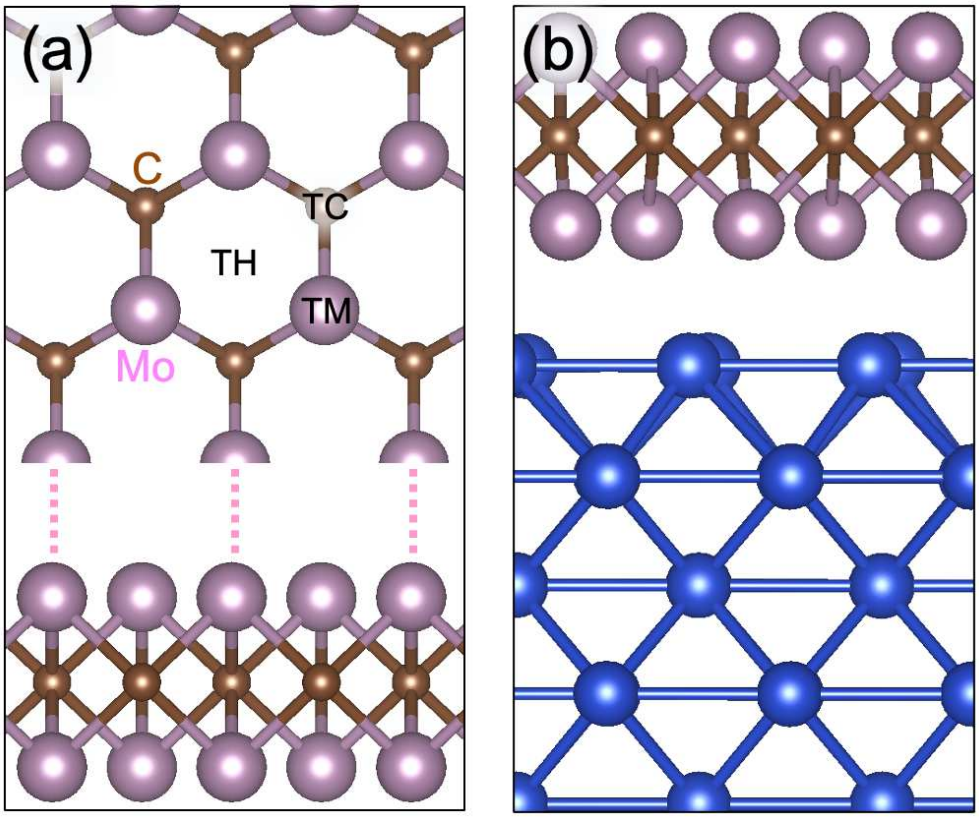

FIG. 1. (Color online) Atomic structures of (a) Mo_2C and (b) Mo_2C on a metal substrate. The pink, brown, and blue balls represent Mo, C, and substrate atoms, respectively. In (a), hydrogen absorption sites are denoted by TH, TC, and TM, which are on-top of a hexagonal center, C atom, and Mo atom, respectively.

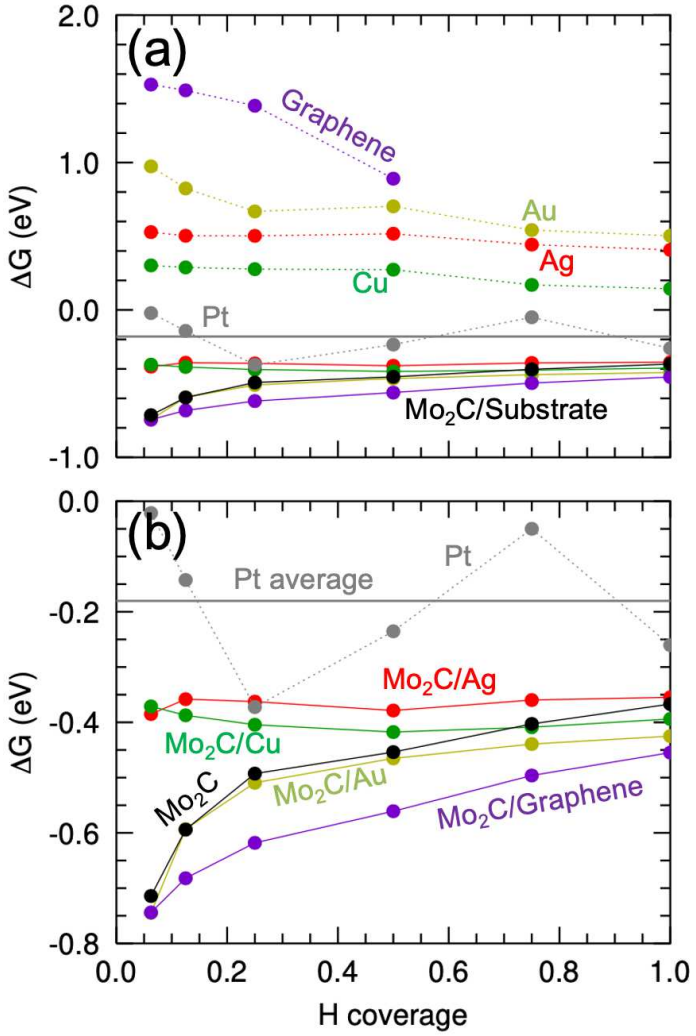

FIG. 2. (Color online) The variation of ΔG with respect to hydrogen coverage. The violate, dark yellow, red, green, and gray dotted lines are the results for the graphene, Au, Ag, Cu, and Pt catalysts, respectively, and the corresponding solid lines are the results for the Mo_2C on each substrate. The black line represents the isolated Mo_2C, and the horizontal gray line is the averaged ΔG for the Pt catalyst, which is considered to have the optimal ΔG. We magnified the energy window from -0.8 to 0.0 eV in (b), which is the ΔG region of Mo_2C.

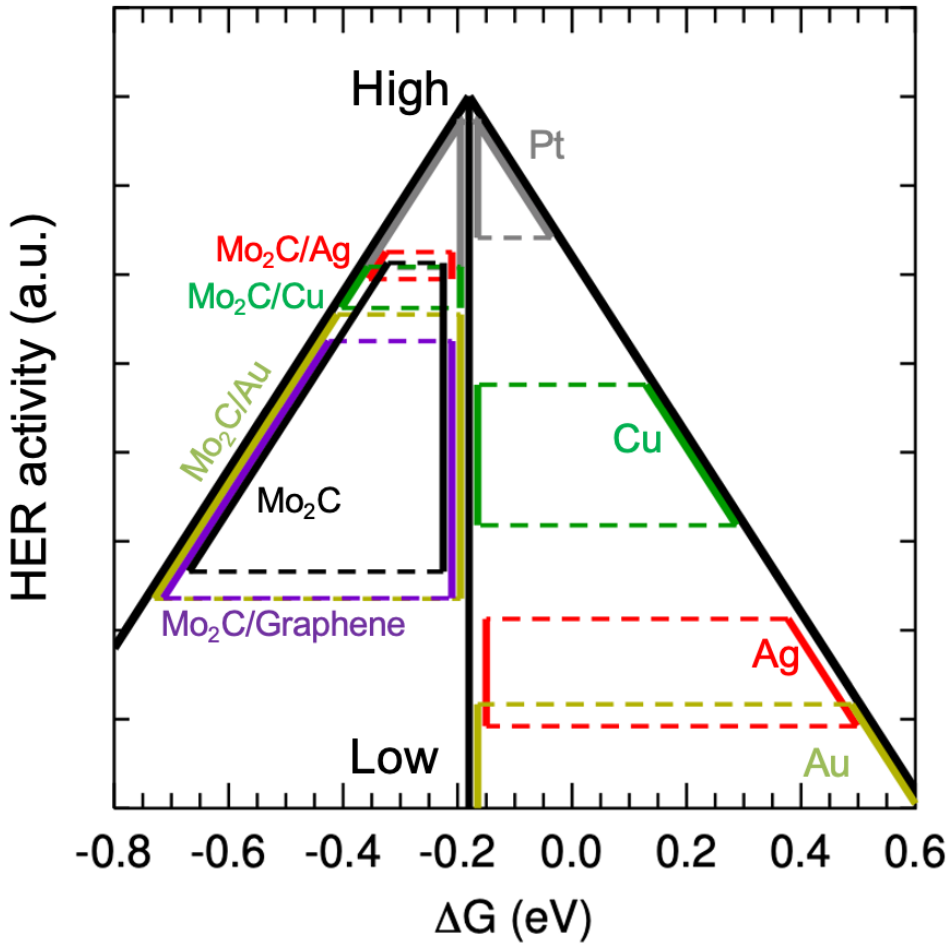

FIG. 3. (Color online) The HER activity for the catalysts Pt (gray), Cu (green), Ag (red), and Au (dark yellow). The HER activity of the Mo_2C on the corresponding substrates are shown. The vertical black line at -0.18 eV represents the optimal value, and the activity of the catalysts are compared on the vertical line. A higher position on the line represents higher HER activity.

	w/o H	w/ H	
	Mo	Mo nearby H	H
Mo_2C	0.566 (5.434)	0.658 (5.342)	-0.453 (1.453)
Mo_2C/Ag	0.498 (5.502)	0.605 (5.395)	-0.457 (1.457)
Mo_2C/Cu	0.508 (5.492)	0.604 (5.396)	-0.451 (1.451)
Mo_2C/Au	0.558 (5.442)	0.657 (5.343)	-0.455 (1.455)

Table 1. The effective charge of the Mo and H atoms in the isolated Mo_2C and Mo_2C on Ag (Mo_2C/Ag), Cu (Mo_2C/Cu), and Au (Mo_2C/Au) substrates obtained from Bader charge analysis. The numbers in parentheses are the number of valence electrons on the corresponding atom. The second column shows the charges and number of valence electrons of the Mo atoms before H absorption, and the third and fourth columns are the values for the Mo atoms that are the nearest neighbors of the H atom and H atom, respectively, after H absorption.

REFERENCE

[1] J. J. Song, C. Wei, Z. F. Huang, C. T. Liu, L. Zeng, X. Wang, and Z. C. J. Xu, Chem. Soc. Rev. **49**, 2196 (2020).

[2] S. Wang, A. L. Lu, and C. J. Zhong, Nano Converg. **8** (2021).

[3] P. De Luna, C. Hahn, D. Higgins, S. A. Jaffer, T. F. Jaramillo, and E. H. Sargent, Science **364**, 350 (2019).

[4] M. Momirlan and T. N. Veziroglu, Int. J. Hydrogen Energ. **30**, 795 (2005).

[5] X. Y. Tian, P. C. Zhao, and W. C. Sheng, Adv. Mater. **31**, 1808066 (2019).

[6] D. Jeon, J. Park, C. Shin, H. Kim, J. W. Jang, D. W. Lee, and J. Ryu, Sci. Adv. **6**, eaaz3944 (2020).

[7] H. M. Sun, Z. H. Yan, F. M. Liu, W. C. Xu, F. Y. Cheng, and J. Chen, Adv. Mater. **32**, 1806326 (2020).

[8] X. L. Tian *et al.*, Science **366**, 850 (2019).

[9] M. Z. Jacobson, W. G. Colella, and D. M. Golden, Science **308**, 1901 (2005).

[10] C. H. Hamann, A. Hamnett, and W. Vielstich, *Electrochemistry* (Wiley-VCH, Weinheim ; New York, 1998).

[11] Y. Jiao, Y. Zheng, K. Davey, and S. Z. Qiao, Nat. Energy **1**, 16130 (2016).

[12] T. F. Jaramillo, K. P. Jorgensen, J. Bonde, J. H. Nielsen, S. Horch, and I. Chorkendorff, Science **317**, 100 (2007).

[13] H. I. Karunadasa, E. Montalvo, Y. J. Sun, M. Majda, J. R. Long, and C. J. Chang, Science **335**, 698 (2012).

[14] C. Tsai, K. R. Chan, J. K. Norskov, and F. Abild-Pedersen, Catal. Sci. Technol. **5**, 246 (2015).

[15] J. Kibsgaard, Z. B. Chen, B. N. Reinecke, and T. F. Jaramillo, Nature Mater. **11**, 963 (2012).

[16] C. Tsai, F. Abild-Pedersen, and J. K. Norskov, Nano Lett. **14**, 1381 (2014).

[17] T. Das, S. Chakraborty, R. Ahuja, and G. P. Das, Chem. Phys. Chem. **20**, 608 (2019).

[18] Y. Hao, Y. T. Wang, L. C. Xu, Z. Yang, R. P. Liu, and X. Y. Li, Appl. Surf. Sci. **469**, 292 (2019).

[19] Y. X. Ouyang, C. Y. Ling, Q. Chen, Z. L. Wang, L. Shi, and J. L. Wang, Chem. Mater. **28**, 4390 (2016).

[20] H. Pan, Nano. Resear. Lett. **11**, 113 (2016).

[21] D. B. Putungan, S. H. Lin, and J. L. Kuo, Phys.l Chem. Chem. Phy. **17**, 21702 (2015).

[22] H. B. Shu, D. Zhou, F. Li, D. Cao, and X. S. Chen, Acs. Appl. Mater. Inter. **9**, 42688 (2017).

[23] C. Wang, Y. Y. Liu, J. Yuan, P. Wu, and W. Zhou, J. Energy Chem. **41**, 107 (2020).

[24] Y. Zhang, X. S. Chen, Y. Huang, C. Zhang, F. Li, and H. B. Shu, J. Phys. Chem. C **121**, 1530 (2017).

[25] Z. Ling, C. E. Ren, M. Q. Zhao, J. Yang, J. M. Giammarco, J. S. Qiu, M. W. Barsoum, and Y. Gogotsi, Proc. Nat. Acad. Sci. USA **111**, 16676 (2014).

[26] M. Naguib, V. N. Mochalin, M. W. Barsoum, and Y. Gogotsi, Adv. Mater. **26**, 992 (2014).

[27] X. F. Wang, X. Shen, Y. R. Gao, Z. X. Wang, R. C. Yu, and L. Q. Chen, J. Am. Chem. Soc. **137**, 2715 (2015).

[28] H. Pan, Sci. Rep. **6**, 32531 (2016).

[29] C. Y. Tang, A. K. Sun, Y. S. Xu, Z. Z. Wu, and D. Z. Wang, J. Power Sources **296**, 18 (2015).

[30] Y. D. Yu, J. Zhou, and Z. M. Sun, Adv. Funct. Mater. **30**, 2000570 (2020).

[31] A. D. Handoko, K. D. Fredrickson, B. Anasori, K. W. Convey, L. R. Johnson, Y. Gogotsi, A. Vojvodic, and Z. W. Seh, Acs. Appl. Energ. Mater. **1**, 173 (2018).

[32] Z. W. Seh, K. D. Fredrickson, B. Anasori, J. Kibsgaard, A. L. Strickler, M. R. Lukatskaya, Y. Gogotsi, T. F. Jaramillo, and A. Vojvodic, Acs. Energy Lett. **1**, 589 (2016).

[33] J. Wan, J. B. Wu, X. Gao, T. Q. Li, Z. M. Hu, H. M. Yu, and L. Huang, Adv. Funct. Mater. **27**, 1703933 (2017).

[34] H. X. Ang, H. T. Tan, Z. M. Luo, Y. Zhang, Y. Y. Guo, G. L. Guo, H. Zhang, and Q. Y. Yan, Small **11**, 6278 (2015).

[35] B. Ding, W. J. Ong, J. Z. Jiang, X. Z. Chen, and N. Li, Appl. Surf. Sci. **500**, 143987 (2020).

[36] H. J. Freund and G. Pacchioni, Chem. Soc. Rev. **37**, 2224 (2008).

[37] L. Giordano and G. Pacchioni, Acc. Chem. Res. **44**, 1244 (2011).

[38] G. Pacchioni and H. Freund, Chem. Rev. **113**, 4035 (2013).

[39] P. Hohenberg and W. Kohn, Phys. Rev. B **136**, B864 (1964).

[40] W. Kohn and L. J. Sham, Phys. Rev. **140**, 1133 (1965).

[41] J. P. Perdew, K. Burke, and M. Ernzerhof, Phys. Rev. Lett. **77**, 3865 (1996).

[42] G. Kresse and J. Furthmuller, Comp. Mater. Sci. **6**, 15 (1996).

[43] P. E. Blochl, Phys. Rev. B **50**, 17953 (1994).

[44] G. Kresse and D. Joubert, Phys. Rev. B **59**, 1758 (1999).

[45] J. Greeley, T. F. Jaramillo, J. Bonde, I. B. Chorkendorff, and J. K. Norskov, Nature Mater. **5**, 909 (2006).

[46] S. Zhou, X. W. Yang, W. Pei, N. S. Liu, and J. J. Zhao, Nanoscale **10**, 10876 (2018).

[47] H. Lou, T. Yu, J. N. Ma, S. T. Zhang, A. Bergara, and G. C. Yang, Phys. Chem. Chem. Phys. **22**, 26189 (2020).

[48] R. Parsons, Trans. Faraday Soc. **54**, 1053 (1958).

[49] B. E. B. Coway, J. O. M., J. Chem. Phys. **26**, 532 (1957).

[50] H. Gerischer, Bull. Soc. Chim. Belg. **67**, 506 (1958).

[51] W. C. Sheng, M. Myint, J. G. G. Chen, and Y. S. Yan, Energ. Environ. Sci. **6**, 1509 (2013).

[52] J. K. Norskov, T. Bligaard, A. Logadottir, J. R. Kitchin, J. G. Chen, S. Pandelov, and J. K. Norskov, J. Electrochem. Soc. **152**, J23 (2005).

[53] J. Greeley, J. K. Norskov, L. A. Kibler, A. M. El-Aziz, and D. M. Kolb, Chem. Phys. Chem. **7**, 1032 (2006).

[54] J. O. Sofo, A. S. Chaudhari, and G. D. Barber, Phys. Rev. B **75**, 153401 (2007).

[55] J. Bang and K. J. Chang, Phys. Rev. B **81**, 193412 (2010).

[56] D. H. Choe, J. Bang, and K. J. Chang, New J. Phys. **12**, 125005 (2010).

[57] J. Bang, S. Meng, Y. Y. Sun, D. West, Z. G. Wang, F. Gao, and S. B. Zhang Proc. Nat. Acad. Sci. USA **110**, 908 (2013).

[58] S. Y. Li, Y. Wang, H. Wang, Q. Y. Zhang, Z. Z. Zhang, and H. Liu, J. Appl. Electrochem .**51**, 1109 (2021).

[59] X. X. Zhao *et al.*, Adv. Mater. **31**, 1808343 (2019).